Use of a Reactor Network Model in the Design and Operation of a New Type of Membrane Wall Entrained Flow Gasifier

ARTICLE *in* ENERGY & FUELS · JULY 2013

Impact Factor: 2.79 · DOI: 10.1021/ef401451f

5 AUTHORS, INCLUDING:

Zhiwei Yang

12 PUBLICATIONS **48** CITATIONS

SEE PROFILE

Zhe Wang

Tsinghua University

45 PUBLICATIONS **366** CITATIONS

SEE PROFILE

Yuxin Wu

Tsinghua University

60 PUBLICATIONS **262** CITATIONS

SEE PROFILE

Zheng Li

Tsinghua University

139 PUBLICATIONS **1,442** CITATIONS

SEE PROFILE

energy&fuels

Article

pubs.acs.org/EF

Use of a Reactor Network Model in the Design and Operation of a New Type of Membrane Wall Entrained Flow Gasifier

Zhiwei Yang,[†] Zhe Wang,*[,†] Yuxin Wu,[‡] Zheng Li,[†] and Weidou Ni[†]

[†]State Key Lab of Power Systems, Department of Thermal Engineering, Tsinghua University, Beijing, China 100084

[‡]Key Laboratory for Thermal Science and Power Engineering of Ministry of Education, Department of Thermal Engineering, Tsinghua University, Beijing 100084

ABSTRACT: China is developing a new type of slurry-feed membrane wall entrained flow gasifier with two-stage oxygen supply in order to improve facility availability and efficiency. Detailed modeling can contribute to obtaining an in-depth understanding of the gasifier and achieving optimal design and operation. In this work, a computationally efficient reactor network model was developed. Available industrial data from a single-stage version of this type of gasifier was used to validate the model. Good agreement was observed in carbon conversion, syngas composition, and steam production in the membrane wall, suggesting that the model was able to provide accurate prediction, including gasifier outlet parameters and internal heat transfer rate. The impact of the five most important parameters on the gasifer performance—the location of second-stage oxygen injectors, the fraction of the second-stage oxygen in total oxygen fed to the gasifier, the thickness of the refractory lining on the membrane wall inner surface, the water tube diameter, and the width of the fins which links the tubes—was investigated. Optimized design and operation guidelines for improving operational economy and availability were provided.

1. INTRODUCTION

Gasification is an important technology in converting coal into power, chemicals, hydrogen, or transportation fuels, and also in precombustion carbon capture from coal.[1] Over the past few decades, experience of the gasification industry showed that the relatively low availability of gasifiers compared with pulverized coal boilers impeded the wide application of current gasification technologies. For improving availability, Tsinghua University (THU) developed its first generation slurry-feed membrane wall gasifier in 2012.[2−5] Operational experience indicates that it has higher availability and improved feedstock flexibility compared with slurry-feed gasifiers with a refractory wall, due to the long lifetime and high temperature resistance of the membrane wall. Moreover, the heat loss through the membrane wall is almost the same level as that in a refractory wall gasifier, which means the efficiency change is very small. Currently, Tsinghua University is designing its second generation gasifier with a two-stage oxygen supply. The design of staged oxygen supply, which has been adopted in the THU oxygen-staged refractory wall gasifier,[6,7] can achieve enhanced carbon conversion and prolonged nozzle lifetime.[8,9]

Table 1 shows a comparison between the newly designed oxygen-staged membrane wall gasifier (OSMWG) and other commercially available membrane wall gasifiers. Distinct differences in flow direction and configuration can be seen in these gasifiers. It suggests that the new gasifier has unique features in the flow, reaction, and heat transfer processes compared with other gasifiers. For developing this new gasifier, it is necessary to obtain an in-depth understanding of its operational characteristics through detailed modeling and optimize important design and operational parameters based on the understanding.

Modeling entrained flow gasifiers is a challenge due to the associated complex and highly coupled physical and chemical processes. Numerous gasifier models have been proposed, which can be divided into four groups: zero-dimensional thermodynamic models,[10−12] one-dimensional kinetic models,[13−16] two- or three-dimensional computational fluid dynamics (CFD) models,[8,17−22] and reactor network models (RNMs).[23−26] Zero- and one- dimensional models, which are simple and convenient, can well predict gasifier outlet parameters, such as the temperature and composition of the produced syngas. But due to the considerable simplification in the flow structure, they cannot offer a reasonable gasifier internal temperature distribution, which is critical for slag layer thickness estimation on the membrane wall. With comprehensive CFD models, detailed flow fields can be obtained, but they require a large amount of computational resources. When they are combined with overall gasification process modeling or used for dynamic simulation, the computational time can hardly be acceptable. RNMs, which capture the main flow features and

Table 1. Characteristics of Commercially Available Membrane Wall Entrained Flow Gasifiers

gasifier	flow	feed	oxidant	stages	water tube arrangement
OSMWG	down	slurry	O_2	two stage oxygen	vertical
Shell gasifier	up	dry	O_2	one stage	vertical
GSP gasifier	down	dry	O_2	one stage	helical
MHI gasifier	up	dry	air	two stage coal	vertical

Received: July 28, 2013
Revised: September 19, 2013
Published: September 24, 2013

   dx.doi.org/10.1021/ef401451f | *Energy Fuels* 2013, 27, 6322−6332

use various ideal chemical reactors to represent different physical areas, are considered to be an affordable solution.

In this work, a RNM for the newly designed oxygen-staged membrane wall gasifier was developed and validated. Several of the most important parameters to gasifier performance were identified and their impacts to gasifier design and operation were investigated. On the basis of the modeling results, optimized design and operational guidelines for improving operational economy and safety were provided

2. OXYGEN-STAGED MEMBRANE WALL GASIFIER

Figure 1 shows a schematic of an oxygen-staged membrane wall gasifier. The main components of the gasifier are the reactor,

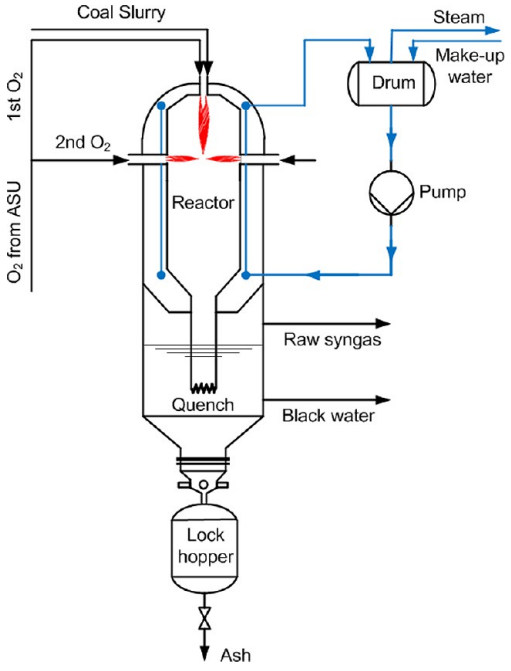

Figure 1. A schematic of the THU membrane wall gasifier.

water quench, steam drum, water-circulating pump, and slag lock hopper. Part of the oxygen is fed into the reactor through a top nozzle with coal slurry, while the remaining oxygen (hereafter referred to as secondary oxygen) is introduced through three horizontal injectors mounted at the same height from the side wall. Saturated water from the steam drum is pumped into the bottom of the membrane wall, absorbs heat, and flows out from the top with a small amount of steam and returns to the steam drum, in which steam and water are separated. Syngas and molten slag produced in the reactor flow into the water quench, in which the syngas flows upward through the water, and the solidified slag is discharged into the lock hopper.

Figure 2 showed the detailed structure of the gasifier wall. The whole gasifier wall consists of a membrane wall, a refractory lining on the inner surface of the membrane wall, an annular chamber filled with high pressure protection gas (usually nitrogen), and a steel vessel. The membrane wall is composed of a group of vertical water tubes, which are connected with each other by tube fins. During operation, because operating temperature is higher than slag melting temperature, a slag layer, which consists of a molten slag layer and a solid slag layer, forms on the refractory lining and acts as

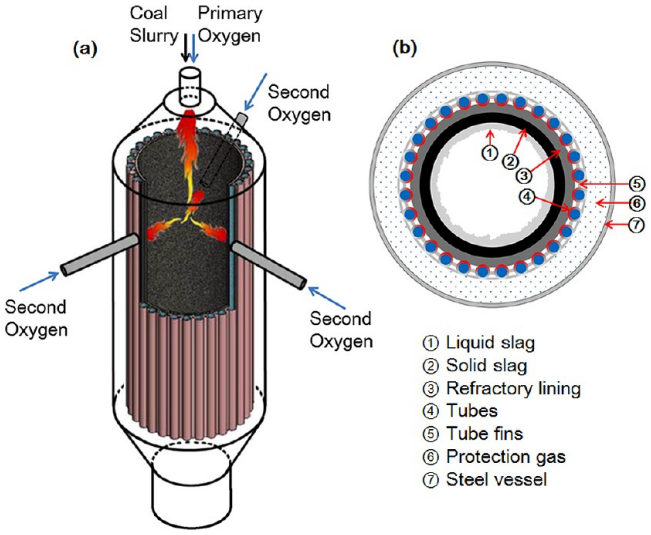

Figure 2. Representation of detailed structures of the gasifier wall: (a) overview of the gasifier reactor with emphasis on membrane wall and (b) horizontal section of the gasifier wall.

additional thermal resistance in the heat transfer through the wall.

3. REACTOR NETWORK MODEL

3.1. Reactor Network Configuration. Establishment of a RNM requires a rational division of the physical space inside the gasifier chamber, which should be based on a deep understanding of internal flow structure of the gasifier. In the current work, the detailed flow field information computed by a comprehensive three-dimensional CFD model for an oxygen-staged refractory wall gasifier was adopted.[8]

On the basis of the CFD modeling results,[8] the physical space in the gasifier chamber can be divided into eight zones as shown in Figure 3: Internal Recirculation Zone (IRZ), External Recirculation Zone in stage 1 (ERZ1), Jet Expansion Zone in stage 1 (JEZ1), External Recirculation Zone in stage 2 (ERZ2), Horizontal Jet Zone (HJZ), Central Mixing Zone (CMZ), Jet Expansion Zone in stage 2 (JEZ2), and Downstream Zone (DSZ), wherein stage 1 and stage 2 represent the physical space above and below the height of the horizontal injectors, respectively.

The central jet expansion zones are formed due to the high speed flow from the top and are accompanied by gas recirculation. The HJZ is composed of three secondary oxygen streams which gather at the centerline and produce the CMZ. Part of the recirculation gas is entrained into the HJZ, the other part flows into the top area, and is eventually returned to the central jets. Geometry parameters of the above zones are summarized in Table 2.

Due to the intensive mixing in IRZ, ERZ1, ERZ2, and CMZ, these zones are modeled by well-stirred reactors (WSR), while JEZ1, JEZ2, HJZ, and DSZ are modeled by plug-flow reactors (PFRs). The configuration of the corresponding reactor network is shown in Figure 3. The gas and particle flow rates between different zones are determined according to the CFD modeling results.

The governing equations for describing the gas−solid reaction flow in plug-flow reactors are summarized in Table 3. They are based on following assumptions: (1) a mean diameter was used for all particles, and (2) particle drying and

dx.doi.org/10.1021/ef401451f | Energy Fuels 2013, 27, 6322−6332

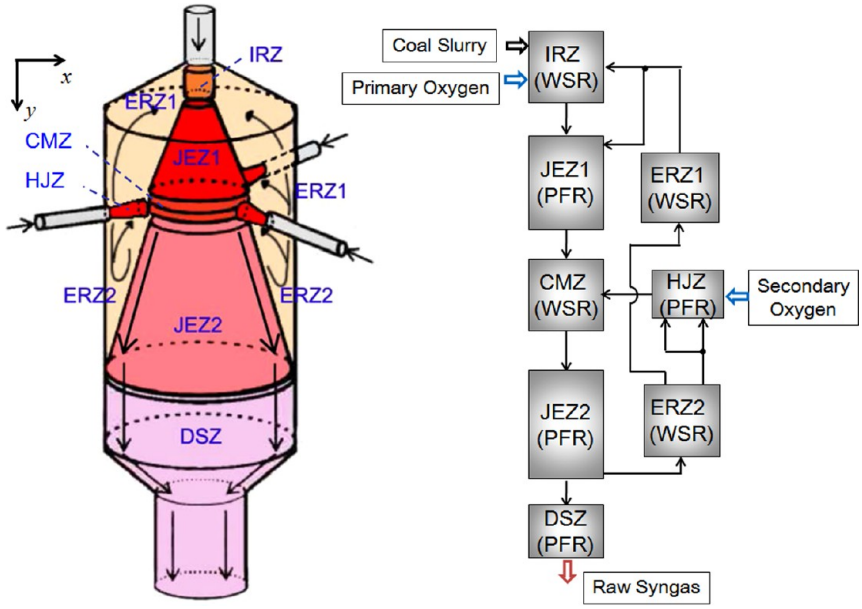

Figure 3. Representation of the physical area division inside the gasifier (on the left) and the organization of the reactor network model (on the right).

Table 2. Geometry Parameters of the Physical Zones inside the Gasifier

zone	D inlet (m)	D outlet (m)	length (m)	volume (m^3)
IRZ	0.32	0.32	0.32	0.026
ERZ1			1.571	3.109
JEZ1	0.32	0.8063	1.251	0.331
ERZ2			2.7155	2.707
HJZ	0.2[a]	0.2[a]	0.464[a]	0.015 × 3
CMZ	0.7477	0.7477	0.2	0.088
JEZ2	0.8063	1.676	2.7155	3.284
DSZ	1.676	0.58	3.3435	5.944

[a]The diameter and length are for each horizontal stream zone.

Table 3. Governing Equations for a Plug Flow Reactor

conserved quantity	expression
gas species mass	$-\partial F_{g,i}/\partial y + AS_{g,i} = 0$
particle phase mass	$-\partial F_p/\partial y + AS_p - \dot{m}_{slagging} = 0$
carbon in particles mass	$-\partial(F_p X_C)/\partial y + AS_C = 0$
gas phase energy	$\partial(F_g h_g)/\partial y + A(\ddot{Q}_{homo} + (1 - f_Q)\ddot{Q}_{hete}) + \dot{Q}_{conv,p\to g} - \dot{Q}_{conv,g\to w} = 0$
solid phase energy	$\partial(F_p h_p)/\partial y + Af_Q\ddot{Q}_{hete} - \dot{Q}_{conv,p\to g} - \dot{Q}_{rad,p\to w}\dot{Q}_{rad,p\to p} - \dot{m}_{slagging}h_p = 0$

devolatilization are assumed to be completed at the outlet of IRZ. When replacing $\partial/\partial y$ with $1/L_{WSR}$, these governing equations can also be applied to well-stirred reactors.

The chemical reaction and heat transfer source terms in Table 3 are determined by a chemical reaction submodel and a heat transfer submodel, which are not presented here since they have been extensively reported in the literature.[27] For a WSR, the species concentrations and temperature at the exit of the reactor are used to calculate these source terms, while for a PFR, they change with y.

Determination of the ash deposition rate on the wall, $\dot{m}_{slagging}$, is challenging due to the complexity of the physics in the ash particle−wall interaction; factors determining the fate of ash particles are still under investigation.[28−33] In the current study, the particle impact rate on the wall provided by the CFD model was used, and the correlation between gasifier height and $\dot{m}_{slagging}$ can be expressed as follows:

$$\dot{m}_{slagging}(y) = 23.5F_{ash}y^* \exp(-y^*/0.2) \quad (1)$$

It should be noted that the above crude approximation may introduce inaccuracy in slag simulation, but since the ash deposition rate mainly affects the liquid slag thickness and liquid slag only accounts for a small part in the total slag layer in a membrane wall gasifier,[27,33−35] this inaccuracy is considered to be acceptable in the current study. A comprehensive submodel for the ash particle capture is left for future development.

3.2. Slag Layer Model. Figure 4 showed the representation of heat fluxes through the slag layer and the gasifier wall. In membrane wall gasifiers, the slag layer strongly affects the heat transfer toward the wall, due to its large thermal resistance compared to the membrane wall.[33−38] Therefore, the slag layer model has a decisive effect on the accuracy of the heat transfer calculation.

In the RNMs built by Monaghan et al.[23−25] and Gazzani et al.,[26] the two phase slag layer structure was simplified as a single molten phase layer. Although the simplification greatly reduces the cost of calculation, it tends to underestimate the slag layer thickness.[26] In our previous work, a liquid−solid two phase model[34] was adopted in the RNM, and it was found that the convergence time was still acceptable. Therefore, in the present work, the same slag model was applied. In addition, the establishment of the two-layer slag model was based on following key assumptions: (1) The transitional temperature between the solid and liquid slag layers is the temperature of ash critical viscosity, T_{cv}. (2) The flow of liquid slag is Newtonian, and the flow at temperatures below T_{cv} is negligible. (3) The temperature profile across the slag layer is linear.

3.3. Membrane Wall Thermal Model. Due to the high convection heat transfer rate inside the water tubes, the heat transfer in the radial direction through a water tube can be

dx.doi.org/10.1021/ef401451f | Energy Fuels 2013, 27, 6322−6332

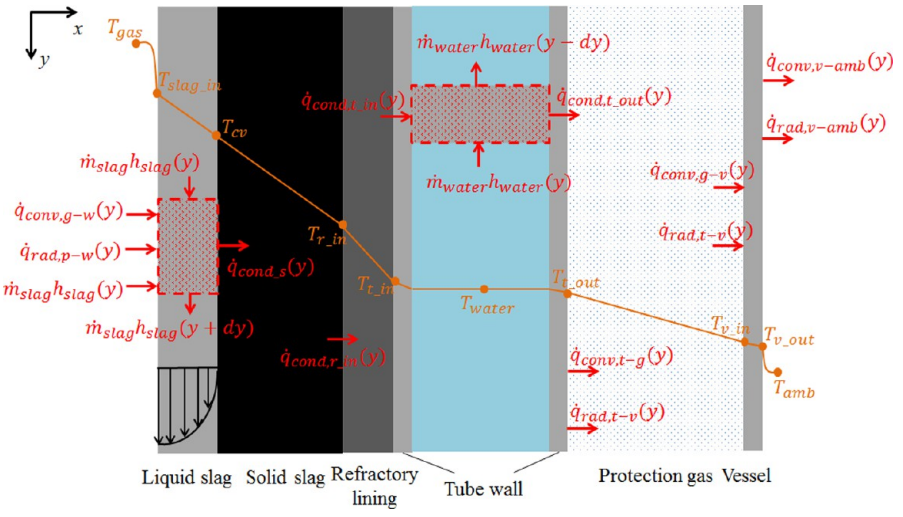

Figure 4. Representation of heat fluxes transferred from the gas and particle side toward the outside environment through the slag layer and gasifier wall.

simplified as a heat transfer problem through an equivalent extended fin, as shown in Figure 5. The same approach was

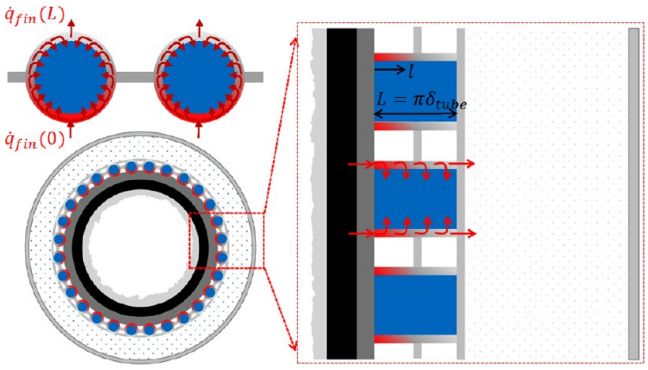

Figure 5. Representation of the equivalent fin model: (a) realistic heat transfer pathways through water tubes, (b) horizontal section of the gasifier wall, and (c) horizontal section of equivalent membrane wall and heat transfer pathways in the equivalent model.

used in the Shell gasifier model built by Gazzani et al.,[26] and the calculated tube temperature in their model is consistent with Shell process experiences reported in the literature.[1]

In this approach, each tube is represented by a pair of equivalent fins. The thickness of each fin equals the tube thickness, and fin length equals half the tube circumference. Every pair of equivalent fins is connected by tube fins. According to heat transfer theories for extended fins,[39] the distribution of temperature and heat flux along a fin can be obtained using eqs 2 and 3, respectively. The excess temperature in eq 2 is written as $\theta(l) = T(l) - T_\infty$, and m in eq 3 is written as $m = (hP/kA_c)^{1/2}$.

$$\frac{\theta(l)}{\theta_0} = \frac{(\theta_L/\theta_0)\sinh(ml) + \sinh(m(L-l))}{\sinh(mL)} \quad (2)$$

$$q_{fin}(l) = -kA_c m\left[\frac{\theta_L\cosh(ml) - \theta_0\cosh(m(L-l))}{\sinh(mL)}\right] \quad (3)$$

The two-phase convection heat transfer coefficient inside water tubes was calculated using a correlation proposed by Steiner and Taborek,[40] which accounted for convective and nucleate heat transfer and is written as eq 4. The method for calculating the parameters in this equation was reported in the literature.[23]

$$h = [(h_{nb,0}F_{nb})^3 + (h_{Lt}F_{tp})^3]^{1/3} \quad (4)$$

3.4. Model Input. The oxygen-staged membrane wall gasifier operates at an elevated pressure of 4.0 MPa. The coal feeding rate is 700t/d. The coal slurry concentration is 60%. The ratio of mass flow rate of oxygen to coal under is 0.93. The total cooling water flow rate in the tubes is 220.9t/h, and the pressure in the tubes is 3.8 MPa. The coal and ash properties are summarized in Table 4. Geometry parameters and thermal properties for the membrane wall are shown in Table 5. The model was developed and solved in Aspen Custom Modeler (AspenTech, Massachusetts, USA).

Table 4. Shenfu Coal Analysis and Ash Properties Used on the Model

	coal analysis
proximate analysis (%) (as-received basis)	FC, 58.10; V, 33.39; moisture, 1.9; ash, 6.61
ultimate analysis(%) (dry basis)	C, 74.39; H, 4.36; O, 13.08; N, 0.92; S, 0.51; ash, 6.74
HHV (MJ/kg)	26.26
	ash properties
viscosity (Pa·s)	$8.59 \times 10^{-8}\ e^{(29095/T)}$
T_{cv} (°C)	1150
density (kg/m^3)	2500
specific heat capacity (kJ/kg·K)	1.69
conductivity (W/m/K)	1.89
emissivity	0.83

4. RESULTS AND DISCUSSION

4.1. Model Validation and Sensitivity Analysis. Since the oxygen-staged membrane wall gasifier is still in the design stage, we used the available industrial data of the single-stage slurry-feed membrane wall gasifier operating in Shanxi, China[3] to validate the model by setting the fraction of the secondary oxygen in total oxygen in the model to be 0%. Table 6 shows a

dx.doi.org/10.1021/ef401451f | Energy Fuels 2013, 27, 6322−6332

Table 5. Geometry Parameters and Thermal Properties of the Membrane Wall

parameters	values
refractory lining thickness (m)	0.016
tube thickness (m)	0.006
tube diameter (m)	0.1
tube fin length (m)	0.05
protection gas chamber thickness (m)	0.4
steel vessel thickness (m)	0.06
refractory lining conductivity (W/m·K)	4.0
steel (tube, vessel) conductivity (W/m·K)	40
steel emissivity at 250 and 70 °C	0.24, 0.22
ambient conditions	25 °C, 1.013 bar

Table 6. Comparisons between Model Results and Industrial Operation Data

	syngas composition (%, dry basis)					
	CO	H2	CO_2	T (°C)	CC (%)	steam production in membrane wall (t/h)
model results	41.5	35.7	20.5	1252.9	97.34	1.7
industrial data	42	38	21	1250.0	98	1−1.5

comparison between the industrial data and the RNM results. Good agreement can be observed. The agreement in the steam production in the membrane wall indicates that the model can give a good estimation of the heat fluxes through the wall. In addition, from our simulation, if average slag layer thickness increased by 10 mm, the total steam production will decrease by 34%, indicating that the heat fluxes through the wall rely heavily on the estimation of the slag layer thickness; therefore the agreement of steam production also, to some extent, indicates the validity of the slag flow simulation.

Although the CFD model derived by Wu et al.[8] is for an oxygen-staged refractory wall gasifier, which has some small differences in geometry compared with the newly designed membrane wall gasifier, the results of the model can still offer rough information with regard to the temperature distribution, considering that the operating conditions of the two gasifiers are almost the same. From the CFD model results, the temperature in the flame zones is 1700−2300 °C, in ERZ1 is 1000−1250 °C, and in ERZ2 is 1100−1300 °C. Figure 6a shows the temperature distribution calculated by the RNM with the same operating conditions as in the CFD model. The temperature profile basically agrees with the CFD model results. Further validation will be carried out after the development of the CFD model for the newly designed membrane wall gasifier has been completed.

Figure 6b shows the water tube temperature along the gasifier length, moving from the inside to the outside. As shown, along the tube position direction, temperature variation is large in $0 < l/L < 0.2$, which corresponds to a small sector area of the tube with an angle of about 72°. In other areas, the temperature is almost constant. This distribution is consistent with the results of a three-dimensional water tube heat transfer simulation carried out by Liang.[41]

In order to identify the impact of the modeling assumptions and input parameters on the model results, a sensitivity analysis is performed with the proposed model. Monaghan and Ghoniem[25] have performed a detailed sensitivity study, which shows the influence of various modeling assumptions of a reactor network gasifier model on the calculated carbon conversion and syngas composition. Results indicate that carbon conversion and syngas composition are mainly determined by the inlet ratios of O_2 to C and H_2O to C; the influences of other parameters are very small. In the present paper, the sensitivity of the total slag layer thickness to various input parameters is investigated. Studied input parameters include slag deposition rate (total deposition amount and deposition profile), slag properties (conductivity, density, viscosity, and temperature of critical viscosity T_{cv}), syngas temperature near the wall, and heat transfer rate from syngas to wall and from wall to cooling water. In addition, the influence of variations of RNM configuration on the model results is also studied. As the CFD model for the newly designed membrane wall gasifier has not been developed, the RNM configuration in the present work is based on the CFD model results with respect to the oxygen-staged refractory wall gasifier,[8] which has small differences in geometry compared with the newly designed gasifier. Therefore, a quantitative study is required to show the impact of variations of the RNM configuration on model results.

Figure 7 shows the sensitivity of the total slag thickness at the gasifier outlet to various input parameters. It shows that the

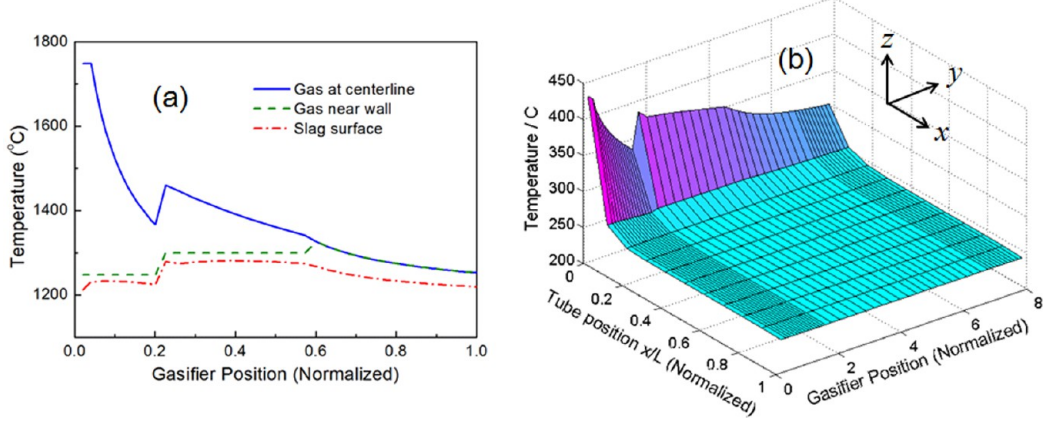

Figure 6. RNM results: (a) temperature distribution inside the gasifier chamber and (b) water tube temperature along the gasifier length, moving from the inside to the outside.

dx.doi.org/10.1021/ef401451f | Energy Fuels 2013, 27, 6322−6332

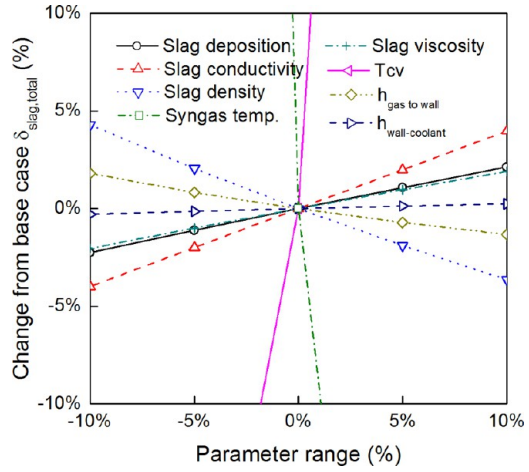

Figure 7. Sensitivity of the slag layer thickness at the gasifier outlet to input parameters.

total slag thickness is mainly determined by syngas temperature and temperature of slag critical viscosity T_{cv}. The impacts of other parameters are very small.

Figure 8 shows the slag thickness profiles under different ash deposition profiles and different RNM configurations. The

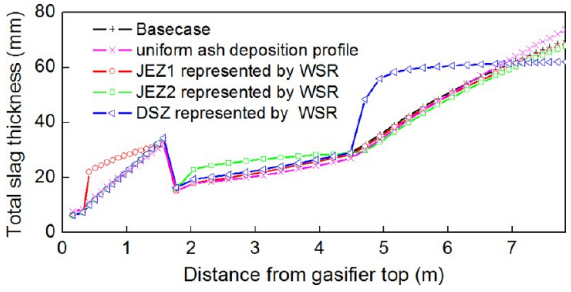

Figure 8. Influence of ash deposition profile and RNM configuration on the slag layer thickness distribution.

uniform deposition profile in the figure means the ash deposition rate along the gasifier height is uniform while the total deposition amount is the same as that calculated by eq 1. It can be found in that the influence of the ash deposition profile on the slag layer thickness is very small, but variation of RNM configuration can lead to a difference. For instance, when the PFR representing DSZ is replaced by WSR, the temperature of the reactor for DSZ becomes uniform. In correspondence, the slag thickness distribution also changes, as shown in Figure 8. Detailed methods for assessing whether a RNM configuration can well approximate the flow field obtained from a CFD model and how to optimize the RNM will be presented in a subsequent paper. However, in the present work, since the optimization study of the gasifier design and operation mainly concerns the varying trends of variables under different conditions rather than the absolute values of these variables, the configuration of the RNM will have small influence on the study results, once it has been decided and remains unchanged during the study.

4.2. Optimization of Design and Operation. On the basis of the RNM, five parameters were investigated: the location of the second stage oxygen injector, the fraction of secondary oxygen in total oxygen, the refractory lining thickness, the water tube diameter, and the tube fin length. The following design is used as the baseline design for comparison: The distance between the second-stage injector and the top nozzle is 2.671 m. The fraction of secondary oxygen in total oxygen is 15%. The refractory lining thickness is 16 mm. The water tube diameter is 10 cm, and the tube fin length is 5 cm. It should be noted that the following discussion about the last three parameters associated with wall design can also apply to other membrane wall gasifiers with vertical tube arrangements.

Before discussing the effect of the parameters, criteria for judging gasifier performance were defined. For operational economy, higher carbon conversion and larger output of effective syngas indicates better economic performance. For operational safety, there are four criteria: the maximum temperature of the refractory lining, whether there is a sharp temperature drop/increase in the refractory lining and the membrane wall, the minimum solid slag layer thickness, and whether there is a sharp drop in the slag layer thickness profile. An extremely high temperature intensifies the chemical interactions between slag and refractory materials, which may cause damage to the refractory lining. Sharp temperature changes in the refractory lining and the membrane wall result in increased thermal stresses and cause damage. A solid slag layer protects the refractory lining against the high temperature, corrosive molten slag. Therefore, an extremely thin solid slag layer lowers the safety margin. Sharp drops in the solid slag thickness profile may cause the solid slag at this place to fall off, which also indicates weakened operational safety.

It should be noted that too large slag thickness may also lead to problems, e.g., blockages at the gasifier outlet, but due to the fact that the slag thickness at the gasifier outlet always stayed within reasonable bounds in the current study, it was not included in the safety assessment.

4.2.1. Location of the Second-Stage Oxygen Injectors. The distance between the second-stage injector and the top nozzle is defined as y_{sec}. Four different values of y_{sec} were chosen for comparison: 0.671 m, 1.671 m, 2.671 m, and 3.671 m. Figure 9 shows the influence of y_{sec} on the internal parameter distributions of the gasifier. As y_{sec} increases, the average temperature along the centerline becomes lower. Due to a lower radiative heat transfer rate, the average slag thickness becomes larger, and overall heat loss through the wall becomes smaller. This leads to less steam production in the membrane wall and a higher gasifier outlet temperature, as shown in Table 7. The lower average temperature has a negative effect on the carbon conversion. However, a larger y_{sec} also leads to larger average particle velocity and longer particle residence time. Long residence time and less heat loss through the wall both have positive effects on the carbon conversion. Therefore, there exists an optimized value for y_{sec} to achieve maximum operational economy. From Table 7, it can be seen that the optimized value is around $y_{sec}/L_{gasifier} = 0.34$.

From the perspective of operational safety, it can be found that a larger y_{sec} results in a sharper temperature drop in the refractory lining and sharper slag thickness drop at the place of the second-stage oxygen injectors. When $y_{sec}/L_{gasifier}$ reaches 0.47, the temperature drop in the refractory lining is bigger than 250 °C, and slag layer thickness drops over 80%, which are both dangerous. Therefore, in an overall view, $y_{sec}/L_{gasifier} = 0.21-0.34$ is suggested considering both economy and safety of the gasifier operation.

4.2.2. Fraction of the Secondary Oxygen in Total Oxygen. The fraction of the secondary oxygen in total oxygen is defined

dx.doi.org/10.1021/ef401451f | Energy Fuels 2013, 27, 6322−6332

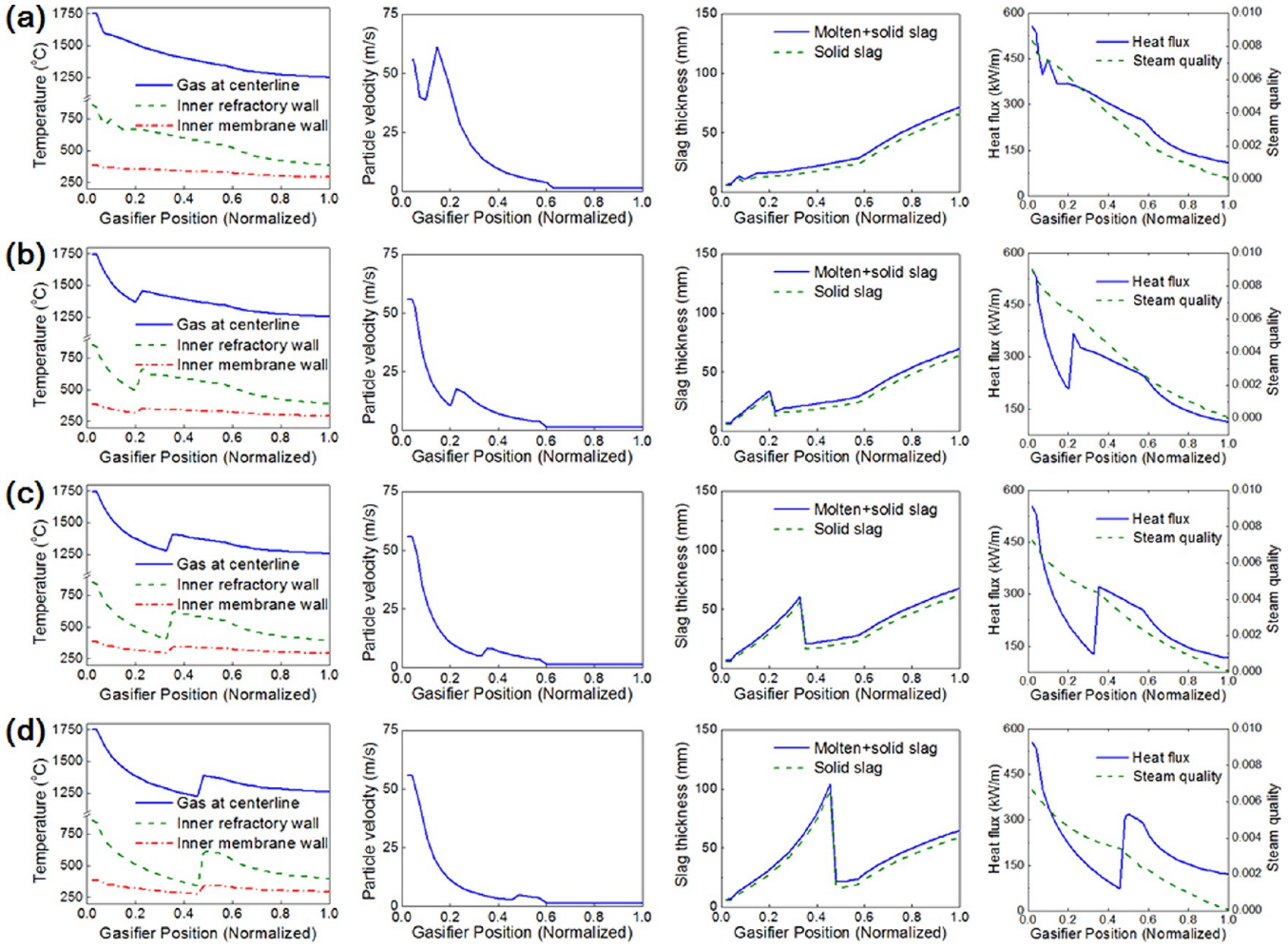

Figure 9. Influence of the secondary oxygen injector position: (a) $y_{sec}/L_{gasifier}$ = 0.09, (b) $y_{sec}/L_{gasifier}$ = 0.21, (c) $y_{sec}/L_{gasifier}$ = 0.34, (d) $y_{sec}/L_{gasifier}$ = 0.47.

Table 7. Gasifier Performance for Different Secondary Oxygen Injector Positions

$y_{sec}/L_{gasifier}$	0.09	0.21	0.34	0.47
steam production (t/h)	1.846	1.726	1.602	1.471
outlet temperature (°C)	1250	1253	1256	1260
carbon conversion (%)	97.24	97.34	97.39	97.38
H_2 + CO (kmol/h)	1922	1926	1927	1926

as R_{sec}. Five different values of R_{sec} were studied: 0%, 5%, 10%, 15%, and 20%. Figure 10 shows the influence of R_{sec} on the gasifier operation. R_{sec} = 0% represents the single-stage membrane wall gasifier. As R_{sec} increases, the temperature in the first stage becomes lower, and the slag thickness in the first stage becomes larger. R_{sec} has little influence on the temperature profile and slag thickness in the second stage. Therefore, the total heat loss through the wall becomes smaller, and less steam is produced in the membrane wall, as shown in Table 8. In addition, a larger R_{sec} results in lower particle velocity at the centerline and hence longer particle residence time. Also, a larger R_{sec} may also cause better mixing. With regard to carbon conversion, a lower average temperature has a negative effect, while a longer residence time and better mixing conditions have a positive effect. Therefore, like the location of the second-stage oxygen injectors, R_{sec} also has an optimized value to achieve maximum operational economy. Table 8 shows that this optimized R_{sec} is around 15−20%.

Considering operational safety, we can see that a higher R_{sec} leads to a lower top flame temperature. Also, a higher R_{sec} means a lower flow speed inside the top nozzle. These will both contribute to an extended nozzle lifetime. According to industrial experience, the lifetime of the top slurry nozzle in an oxygen-staged gasifier is over 50% longer than that of a single-stage GE gasifier. Moreover, as R_{sec} increases, the maximum temperature of the refractory lining becomes lower, and the minimum solid slag thickness is larger. However, at the location of the second-stage injectors, the temperature change in the refractory lining and the slag thickness drop both get sharper. In a general view, around 15% is favorable for R_{sec}.

4.2.3. Refractory Lining Thickness. The refractor lining thickness is defined as L_{refrac}. Four different values of L_{refrac} were investigated: 6 mm, 11 mm, 16 mm, and 21 mm. Figure 11 shows the influence of L_{refrac} on the gasifier operation. As L_{refrac} decreases, the refractory lining temperature becomes lower, and the slag layer becomes thicker. Since the thermal resistance increase of the slag layer compensates for the decline of the thermal resistance of the refractory lining, the temperature at the molten slag surface and the overall heat loss through the wall remain constant. Therefore, L_{refrac} has little effect on the operational economy.

dx.doi.org/10.1021/ef401451f | Energy Fuels 2013, 27, 6322−6332

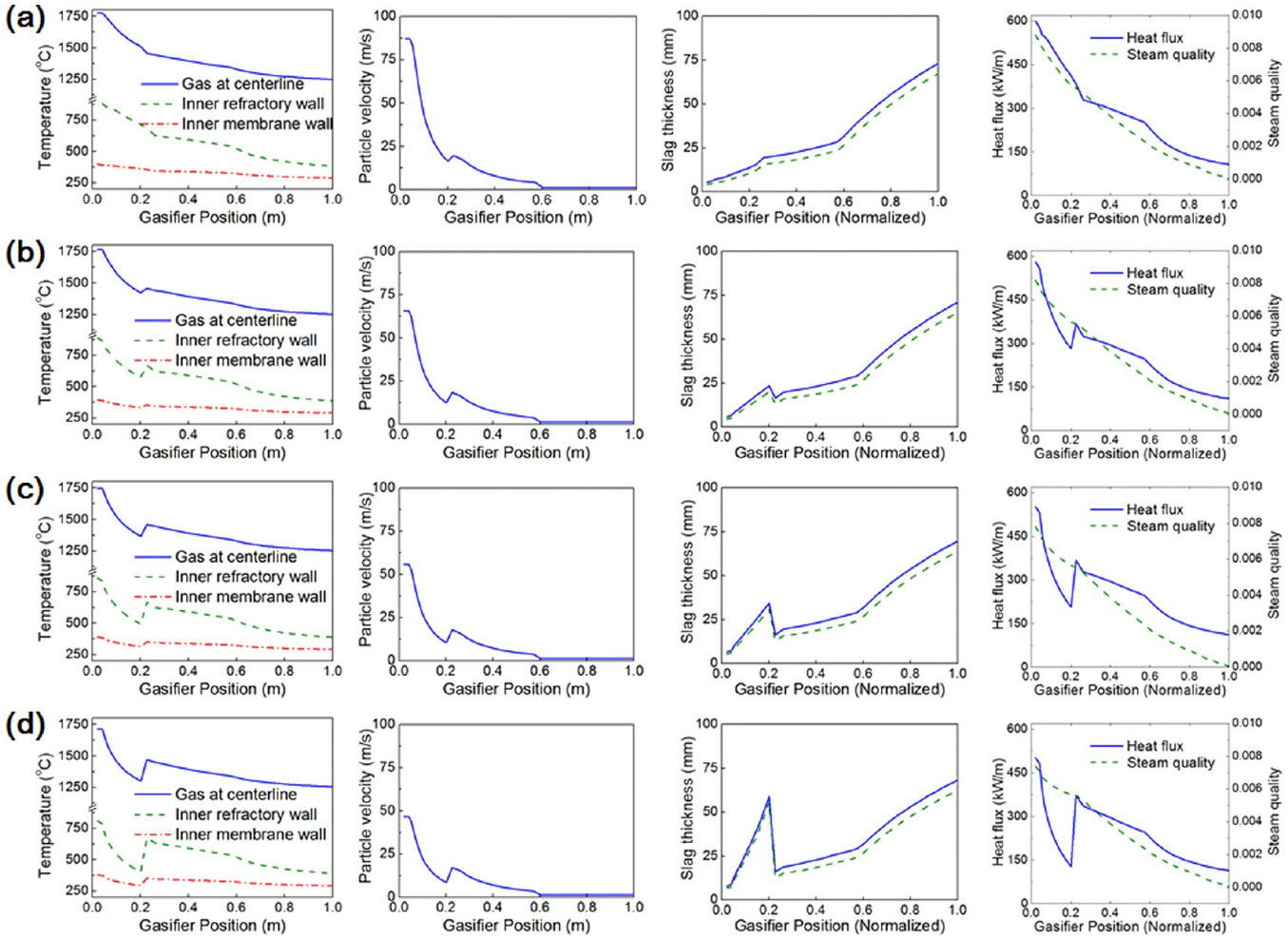

Figure 10. Influence of the secondary oxygen ratio: (a) R_{sec} = 0%, (b) R_{sec} = 10%, (c) R_{sec} = 15%, (d) R_{sec} = 20%.

Table 8. Gasifier Performance for Different Fractions of Secondary Oxygen in Total Oxygen

R_{sec} (%)	0	5	10	15	20
steam production (t/h)	1.944	1.880	1.808	1.726	1.645
outlet temperature (°C)	1248	1249	1251	1253	1255
carbon conversion (%)	97.28	97.30	97.32	97.34	97.34
H_2 + CO (kmol/h)	1920	1922	1924	1926	1926

However, for operational safety, reducing L_{refrac} significantly improves the gasifier performance, because not only does the maximum temperature of the refractory lining decrease as L_{refrac} decreases, the temperature drop at the location of the second-stage injectors also becomes smaller. Therefore, decreasing the refractory lining thickness is highly recommended. But totally removing the lining is not suggested because the protection of the lining is still needed during gasifier startup, when there is little slag deposited on the wall.

4.2.4. Tube Diameter and Fin Length. The tube diameter and fin length are defined as *tube_d* and *fin_L*, respectively. Four different values of *tube_d*, including 12 cm, 10 cm, 8 cm, and 6 cm, and three different values of *fin_L*, including 0 cm, 5 cm, and 10 cm, are studied, while keeping the total mass flow rate of the water in the membrane wall unchanged. Figure 12 shows the influence of *tube_d* and *fin_L* on the gasifier operation. For both parameters, it can be found that the

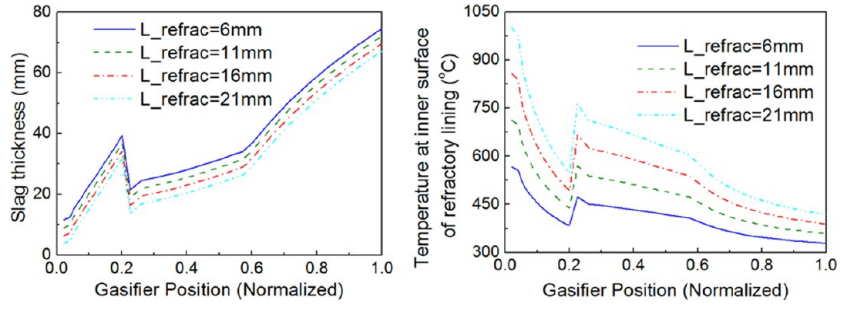

Figure 11. Influence of the refractory lining thickness.

dx.doi.org/10.1021/ef401451f | *Energy Fuels* 2013, 27, 6322−6332

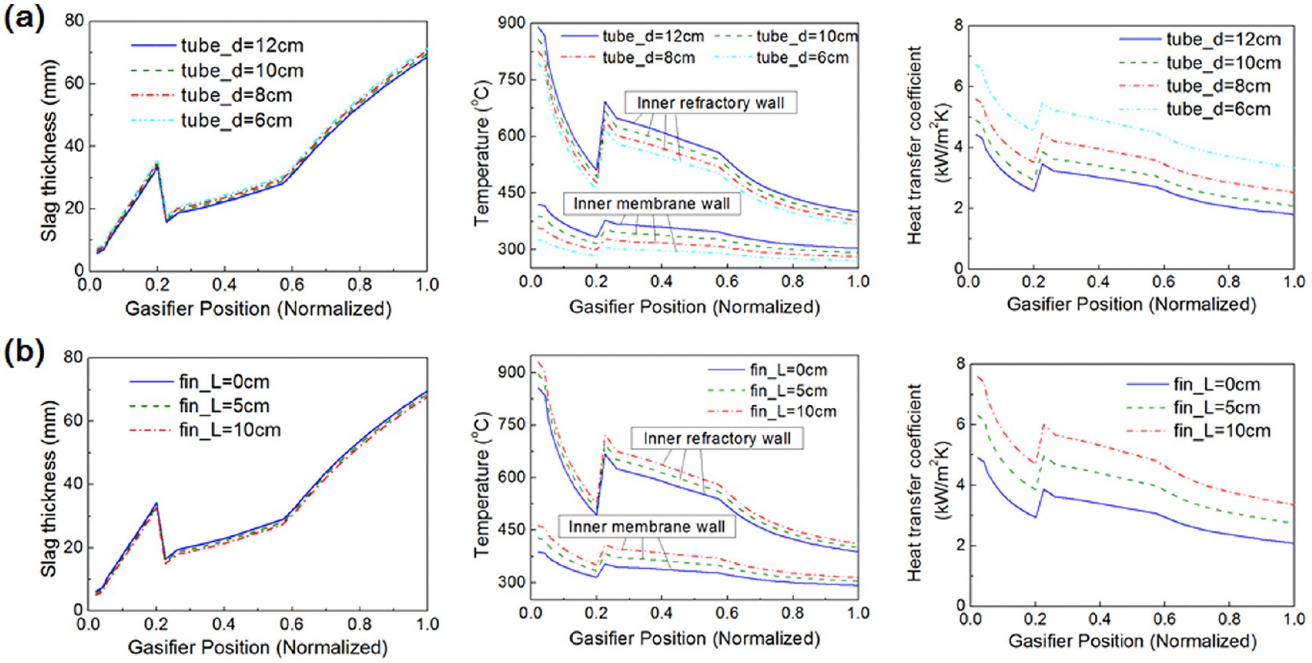

Figure 12. Influence of tube design parameters: (a) tube diameter and (b) fin length.

changes of slag thickness always tend to compensate the thermal resistance variations of the membrane wall. Therefore, these parameters also have little effect on the operational economy.

From the perspective of operational safety, when *tube_d* decreases, the number of tubes increases. Although the mass flow rate of water in each tube decreases, the heat transfer coefficient inside each tube still increases due to smaller *tube_d*. The resulting higher heat transfer rate leads to lower maximum temperature of the refractory lining and membrane wall, hence enhanced operational safety. However, a smaller *tube_d* also causes increased flow resistance and a higher power demand for the water pump.

When *fin_L* increases, the number of tubes decreases; thus the mass flow rate of water and heat transfer coefficient inside each tube both increase. But due to the smaller contacting area between water and tubes, the overall thermal resistance of the membrane wall increases. As a result, a larger *fin_L* leads to a higher maximum temperature of the refractory lining and membrane wall and weakened operational safety. But a larger *fin_L* also means less steel consumption and a lower capital cost for constructing the membrane wall.

5. CONCLUSIONS

A computationally efficient model was developed for a new type of entrained flow gasifier, i.e., oxygen-staged membrane wall gasifier, using a reactor network modeling approach. Calculated syngas composition, carbon conversion, and steam production in the membrane wall all agree well with available industrial data, suggesting that the model has relatively good accuracy on both outlet parameter prediction and estimation of internal heat transfer. Five parameters which are important to gasifier operation were investigated, and the following design and operation guidelines can be concluded:

1. For operational economy, the optimized location for the second-stage injector is around $y_{sec}/L_{gasifier}$ = 0.34. But for operational safety, a small y_{sec} is favorable. In a general view, $y_{sec}/L_{gasifier}$ = 0.21−0.34 is suggested.

2. The optimized fraction of the secondary oxygen in total oxygen for operational economy is around 15−20%. Increasing the fraction of the secondary oxygen can contribute to prolonging the nozzle lifetime and increasing the minimum solid slag layer thickness, but too large of a fraction causes large thermal stress in the refractory lining. In general, a fraction of lower than about 15% is suggested.

3. Decreasing the thickness of the refractory lining can lead to both lower maximum temperature and smaller thermal stress in the refractory lining. It is highly recommended, as long as the protection to the membrane wall during gasifier startup is enough.

4. Decreasing the tube diameter and the fin length can decrease the maximum temperatures of the refractory lining. But care should be taken when changing these parameters because a smaller tube diameter leads to a higher flow resistance in the tubes, while a smaller fin length means a higher capital cost for construction of the membrane wall.

AUTHOR INFORMATION

Corresponding Author

*Tel: +86-13811902238. Fax: 86-10-62795736. E-mail: zhewang@tsinghua.edu.cn.

Notes

The authors declare no competing financial interest.

ACKNOWLEDGMENTS

The work is sponsored by the National Key Basic Research Development Program of China (973 Program, 2010CB227006) and the Science and Technology Fund of State Grid Corporation of China (KJ-2012-627).

NOMENCLATURE

A = Flow area inside reactors in the network, m^2
A_c = area of a cross section of an equivalent fin, m^2
F_{ash} = mass flow rate of total ash in incoming coal
$F_{g,i}$ = mole flow rate of the ith gas species, mol/s

dx.doi.org/10.1021/ef401451f | Energy Fuels 2013, 27, 6322−6332

F_{nb} = nucleate boiling correction factor
f_Q = The portion absorbed by particles in the energy produced by gas-particle reactions
F_{tp} = two-phase multiplier accounting for enhancement of liquid convection by higher velocity of a two-phase flow compared to single-phase flow of liquid
h = convection heat transfer coefficient inside water tubes, kW/m^2/K
h_g = gas phase specific enthalpy, kJ/kmol
h_{Lt} = local liquid-phase convection coefficient based on total flow as liquid, kW/m^2/K
$h_{nb,\,0}$ = local nucleate pool boiling coefficient at a reference heat flux q_0 at the reduced pressure p_r equal to 0.1, kW/m^2/K
h_p = solid phase specific enthalpy, kJ/kg
HHV = high heating value of the coal, MJ/kg
k = conductivity of steel material used for water tubes and gasifier vessel, kW/m/K
l = distance from fin base in an equivalent extend fin
L = length of an equivalent extend fin
L_{WSR} = length of a well-stirred reactor
$\dot{m}_{slagging}$ = slag impinging rate on unit-length wall, kg/m/s
P = perimeter of a cross section of an equivalent fin, m
$\dot{Q}_{conv,p\rightarrow g}$ = heat transfer term for convection between particles and gas, kW/m
$\dot{Q}_{conv,g\rightarrow w}$ = heat transfer term for convection between gas and wall, kW/m
$\dot{Q}_{rad,p\rightarrow w}$ = heat transfer term for radiation between particles and wall kW/m
$\dot{Q}_{rad,p\rightarrow p}$ = heat transfer term for radiation between particles in adjacent zones, kW/m
$\dot{Q}_{homo}$ = heat source of gas-gas reactions, kW/m3
$\dot{Q}_{hete}$ = heat source of gas-particle reactions, kW/m3
S_C = chemical reaction source of carbon in particles, kg/m3/s
$S_{g,i}$ = chemical reaction source of ith gas species, kmol/m3/s
S_p = chemical reaction source of particles, kg/m3/s
T_{cv} = temperature of ash critical viscosity, °C
$T(l)$ = Temperature at position l along an equivalent fin, °C
T_∞ = saturation temperature of the water inside tubes, °C
X_C = mass fraction of carbon in particles
y = distance from gasifier top, m
y^* = normalized distance from gasifier top

Greek Letters

θ = excess temperature, °C

Subscripts

i = index of gas species
g = gas phase
p = particle phase

REFERENCES

(1) Higman, C.; Van der Burgt, M. *Gasification*; Gulf Professional Publishing: Houston, TX, 2008; Vol *10*.
(2) Li, Z.; Han, X.; Meng, L.; Zhai, Y. Comprehension discussion on technology of water-coal slurry gasification. *Zhongdanfei* **2012**, *2*, 7−10 (in Chinese).
(3) Wu, C. Design and operation of coal-slurry membrane wall gasifier. *Mei Huagong* **2012**, *2*, 10−12 (in Chinese).
(4) Wang, Z.; Han, X. Sum-up of project for water-cooled wall gasifier based on coal-water Slurry. *Huafei Gongye* **2012**, *39* (1), 57−62 (inChinese).
(5) Wang, J. Industrialization progress and prospect of coal slurry membrane wall gasification technology. *Nitrogen. Fert. Technol.* **2012**, *33* (4), 17−21 (in Chinese).
(6) Zhang, J.; Hu, W.; Wu, Y.; Lv, J.; Yue, G. Study on the modeling of staged entrained flow gasifier. *Huaxue Gongcheng (Tianjin, China)* **2007**, *35* (3), 14−18 (in Chinese).
(7) Zhang, J.; Wu, Y.; Liu, Q.; Lv, J.; Yue, G. Effect of Second Airflow on Three-Dimensional Velocity Distribution in Staged Coal Gasifier. *Ranshao Kexue Yu Jishu* **2007**, *13* (2), 131−135 (in Chinese).
(8) Wu, Y. X.; Zhang, J. S.; Smith, P. J.; Zhang, H.; Reid, C.; Lv, J. F.; Yue, G. X. Three-Dimensional Simulation for an Entrained Flow Coal Slurry Gasifier. *Energy Fuels* **2010**, *24* (2), 1156−1163.
(9) Wu, Y.; Cai, C.; Zhang, J.; Lv, J.; Yue, G. Numerical investigation of effects of secondary oxygen ratio on performance of staged-entrained flow coal gasfier. *Huagong Xuebao (Chin. Ed.)* **2012**, *63* (2), 369−374 (in Chinese).
(10) Ruprecht, P.; Schafer, W.; Wallace, P. A computer model of entrained coal gasification. *Fuel* **1988**, *67* (6), 739−742.
(11) Bockelie, M. J.; Denison, M. K.; Chen, Z.; Senior, C. L.; Sarofim, A. F. Using Models To Select Operating Conditions for Gasifiers. International Symposium on Utilisation of Coal and Biomass: Energy and Environment, Newcastle, Australia, 2003.
(12) Dai, Z.; Gong, X.; Guo, X.; Liu, H.; Wang, F.; Yu, Z. Pilot-trial and modeling of a new type of pressurized entrained-flow pulverized coal gasification technology. *Fuel* **2008**, *87* (10−11), 2304−2313.
(13) Wen, C.; Chaung, T. Entrainment coal gasification modeling. *Ind. Eng. Chem. Proc. Des. Dev.* **1979**, *18* (4), 684−695.
(14) Vamvuka, D.; Woodburn, E.; Senior, P. Modelling of an entrained flow coal gasifier. 1. Development of the model and general predictions. *Fuel* **1995**, *74* (10), 1452−1460.
(15) Biagini, E.; Bardi, A.; Pannocchia, G.; Tognotti, L. Development of an entrained flow gasifier model for process optimization study. *Ind. Eng. Chem. Res.* **2009**, *48* (19), 9028−9033.
(16) Liu, G. S.; Rezaei, H.; Lucas, J.; Harris, D.; Wall, T. Modelling of a pressurised entrained flow coal gasifier: the effect of reaction kinetics and char structure. *Fuel* **2000**, *79* (14), 1767−1779.
(17) Chen, C.; Horio, M.; Kojima, T. Use of numerical modeling in the design and scale-up of entrained flow coal gasifiers. *Fuel* **2001**, *80* (10), 1513−1523.
(18) Choi, Y.; Li, X.; Park, T.; Kim, J.; Lee, J. Numerical study on the coal gasification characteristics in an entrained flow coal gasifier. *Fuel* **2001**, *80* (15), 2193−2201.
(19) Watanabe, H.; Otaka, M. Numerical simulation of coal gasification in entrained flow coal gasifier. *Fuel* **2006**, *85* (12−13), 1935−1943.
(20) Kumar, M.; Ghoniem, A. F. Multiphysics Simulations of Entrained Flow Gasification. Part I: Validating the Nonreacting Flow Solver and the Particle Turbulent Dispersion Model. *Energy Fuels* **2011**, *26* (1), 451−463.
(21) Kumar, M.; Ghoniem, A. F. Multiphysics Simulations of Entrained Flow Gasification. Part II: Constructing and Validating the Overall Model. *Energy Fuels* **2011**, *26* (1), 464−479.
(22) Ma, J.; Zitney, S. E. Computational Fluid Dynamic Modeling of Entrained-Flow Gasifiers with Improved Physical and Chemical Submodels. *Energy Fuels* **2012**, *26* (12), 7195−7219.
(23) Monaghan, R. F. D. Dynamic reduced order modeling of entrained flow gasifiers. Ph.D. thesis, Massachusetts Institute of Technology, Cambridge, MA, 2010.
(24) Monaghan, R. F. D.; Ghoniem, A. F. A dynamic reduced order model for simulating entrained flow gasifiers: Part I: Model development and description. *Fuel* **2012**, *91* (1), 61−80.
(25) Monaghan, R. F. D.; Ghoniem, A. F. A dynamic reduced order model for simulating entrained flow gasifiers. Part II: Model validation and sensitivity analysis. *Fuel* **2012**, *94* (0), 280−297.
(26) Gazzani, M.; Manzolini, G.; Macchi, E.; Ghoniem, A. F. Reduced order modeling of the Shell−Prenflo entrained flow gasifier. *Fuel* **2013**, *104* (0), 822−837.

(27) Yang, Z.; Wang, Z.; Wu, Y.; Wang, J.; Lu, J.; Li, Z.; Ni, W. Dynamic model for an oxygen-staged slagging entrained flow gasifier. *Energy Fuels* **2011**, *25* (8), 3646−3656.
(28) Shimizu, T.; Tominaga, H. A model of char capture by molten slag surface under high-temperature gasification conditions. *Fuel* **2006**, *85* (2), 170−178.
(29) Shannon, G.; Rozelle, P.; Pisupati, S. V.; Sridhar, S. Conditions for entrainment into a FeO_x containing slag for a carbon-containing particle in an entrained coal gasifier. *Fuel Process. Technol.* **2008**, *89* (12), 1379−1385.
(30) Montagnaro, F.; Salatino, P. Analysis of char−slag interaction and near-wall particle segregation in entrained-flow gasification of coal. *Combust. Flame* **2010**, *157* (5), 874−883.
(31) Ni, J.; Yu, G.; Guo, Q.; Zhou, Z.; Wang, F. Submodel for Predicting Slag Deposition Formation in Slagging Gasification Systems. *Energy Fuels* **2011**, *25* (3), 1004−1009.
(32) Li, S.; Wu, Y.; Whitty, K. J. Ash Deposition Behavior during Char−Slag Transition under Simulated Gasification Conditions. *Energy Fuels* **2010**, *24* (3), 1868−1876.
(33) Benyon, P. Computational modelling of entrained flow slagging gasifiers. Ph.D. thesis, University of Sydney, Sydney, Australia, 2002.
(34) Seggiani, M. Modelling and simulation of time varying slag flow in a Prenflo entrained-flow gasifier. *Fuel* **1998**, *77* (14), 1611−1621.
(35) Ni, J.; Zhou, Z.; Yu, G.; Liang, Q.; Wang, F. Molten Slag Flow and Phase Transformation Behaviors in a Slagging Entrained-Flow Coal Gasifier. *Ind. Eng. Chem. Res.* **2010**, *49* (23), 12302−12310.
(36) Kittel, J.; Hannemann, F.; Mehlhose, F.; Heil, S.; Meyer, B.; Freiberg, T. U. B. Dynamic modelling of the heat transfer into the cooling screen of the SFGT-Gasifier. The 7th International Modelica Conference, Como, Italy, Sep. 20−22, 2009; Linköping University Electronic Press: Linköping, Sweden, 2009; pp 326−334.
(37) Li, B.; Brink, A.; Hupa, M. Simplified Model for Determining Local Heat Flux Boundary Conditions for Slagging Wall. *Energy Fuels* **2009**, *23* (7), 3418−3422.
(38) Yong, S. Z. Multiphase Models of Slag Layer Built-up in Solid Fuel Gasification and Combustion. Dept. of Mechanical Engineering, Massachusetts Institute of Technology: Cambridge, MA, 2010.
(39) Incropera, F. P.; De Witt, D. P. *Fundamentals of Heat and Mass Transfer*; Wiley and Sons, Inc.: New York, 1985
(40) Thome, J. R. *Engineering Data Book III*; Wolverine Tube, Inc.: Decatur, AL, 2006.
(41) Liang, Q. The study on Characteristic of Diffusion Flame and Slag Deposit and Heat transfer in Water Wall Entrained Flow Gasifier. Ph.D thesis, East China University of Science and Technology (ECUST): Shanghai, 2010 (in Chinese).